Clinical & Experimental IMMUNOLOGY

OXFORD

Research Article

The AHNAK induces increased IL-6 production in CD4+ T cells and serves as a potential diagnostic biomarker for recurrent pregnancy loss

Liman Li[1, ID]**, Yuan Liu**[1]**, Ting Feng**[1]**, Wenjie Zhou**[1]**, Yanyun Wang**[1,‡,*] **and Hong Li**[1,‡,*]

[1]Center of Translational Medicine, Key Laboratory of Birth Defects and Related Diseases of Women and Children, Ministry of Education, West China Second University Hospital, Sichuan University, Chengdu, China

‡These authors share senior authorship.

*Correspondence: Yanyun Wang, Center of Translational Medicine, Key Laboratory of Birth Defects and Related Diseases of Women and Children, Ministry of Education, West China Second University Hospital, Sichuan University, Chengdu, China. Email: wangyanyun_hx@foxmail.com; or Hong Li, Center of Translational Medicine, Key Laboratory of Birth Defects and Related Diseases of Women and Children, Ministry of Education, West China Second University Hospital, Sichuan University, Chengdu, China. Email: lihonghx@scu.edu.cn

Abstract

Disorganized maternal–fetal immune tolerance contributes to the occurrence of unexplained recurrent pregnancy loss (RPL). AHNAK is a scaffolding protein participating in the regulation of Ca2+ entry into T cells and the pathophysiology of diverse diseases. We performed differential gene expression analysis in decidual immune cells (DICs) isolated from three patients with RPL and from three healthy controls via RNA-sequencing (RNA-seq), which revealed 407 differentially expressed genes (DEGs). Among these DEGs, we underscored the clinical significance of elevated AHNAK mRNA and protein levels in DICs, peripheral blood mononuclear cells (PBMCs), and decidua of the patients with RPL, suggesting its potential use as a biomarker for the diagnosis of RPL. Especially, the ratios of decidual and blood AHNAK+CD4+ T cells in the CD4+ T cell population were significantly increased in patients with RPL, and the loss of AHNAK was further shown to inhibit interleukin (IL)-6 secretion in the CD4+ Jurkat cell line. Similar patterns were also observed in the clinical decidual and blood specimens. We uncovered that the AHNAK+CD4+ T cells could secrete more IL-6 than that the corresponding AHNAK-CD4+ T cells. Moreover, the frequencies of decidual and blood IL-6+CD4+ T cells in the CD4+ T-cell population were also increased in patients with RPL and showed significant positive correlations with the frequencies of AHNAK+CD4+ T cells. Our findings suggest that the elevated AHNAK expressed by CD4+ T cells may be involved in the immune dysregulation of RPL by increasing IL-6 production, illustrating its potential as a novel intervention target for RPL.

Keywords: recurrent pregnancy loss, AHNAK, IL-6, CD4+ T cell, immune regulation

Abbreviations: AUC, area under the curve; BP, biological processes; CC, cellular components; DEGs, differentially expressed genes; DICs, decidual immune cells; GO, gene ontology; HCs, healthy controls; MF, molecular functions; NK cell, natural killer cell; PBMCs, peripheral blood mononuclear cells; PPI, protein–protein interaction; ROC, receiver operating characteristic; RPL, recurrent pregnancy loss.

Introduction

Recurrent pregnancy loss (RPL) is a devastating experience for most couples. RPL refers to the loss of two or more clinically recognized pregnancies before 20–24 weeks, including embryonic and fetal losses [1]. Several risk factors for RPL have been identified, such as increased maternal age, obesity, poor lifestyles (smoking, excessive alcohol consumption, and stress), anatomical uterine defects, and endometrial dysfunction [2]. Despite its complex etiology, the underlying cause of this condition still cannot be confirmed for more than 50% of couples. Recently, a considerable amount of research has strived to investigate this, with the dysregulated immune systems being a topic of particular interest [3]. On the one hand, dysfunction of T cells, natural killer (NK) cells, γδ T cells, and other immune cells could result in excessive inflammatory responses, perturbing immune equilibrium during early pregnancy. In addition, immune cells are prominent in the decidua and exhibit a close association with invading extravillous trophoblasts and decidual stromal cells. When the function of these cells is disrupted, the processes of placentation, decidualization, and trophoblast invasion will be affected, finally leading to RPL [4, 5].

AHNAK is the largest protein in the body and has pleiotropic functions such as calcium homeostasis, formation of cytoskeletal structure, and muscular regeneration [6]. Although AHNAK is involved in these critical biological processes, it has shown conflicting expression patterns and functions as a tumor promoter or suppressor in various cancers, including ovarian cancer, thyroid carcinoma, and bladder cancer [7–9]. Immunologically, both helper (CD4+) and killer (CD8+) T-cells express high levels of AHNAK after their differentiation and require this molecule for Ca²⁺ entry during an immune response [10, 11]. AHNAK-deficient CD4+ T cells exhibit the low proliferation and low Interleukin(IL)-2 production [12]. Another study demonstrates that IL-4 and

IFN-γ are impaired in AHNAK-KO mice, and this contributes to the impairment of Th1/Th2 immunity [13]. Although AHNAK is constitutively expressed at high levels on human CD4+ T cells and plays a crucial role in the control of Th1/Th2 balance, its biological and functional relevance in RPL remains completely unexplored.

Inflammatory processes may contribute to RPL, possibly through their roles in implantation [14]. The inflammatory event is made possible by the secretion of biological mediators such as IL-12, IL-18, TNF-α, IFN-γ, and IL-6 [14–16]. IL-6 is produced by diverse cells, including monocytes, T cells, B cells, myometrial cells, and endothelial cells [17]. It has been previously shown that maternal serum IL-6 elevation during pregnancy could induce abnormal behavior in offspring in mice, and the human serum IL-6 level is significantly increased in patients with gestational diabetes mellitus [18, 19]. However, the concentration of IL-6 is also reported to be significantly decreased in the supernatants of cultured peripheral blood mononuclear cells (PBMCs) from patients with RPL as compared to that in normal pregnant women during the first trimester [20]. Overall, the duality of IL-6 levels during pregnancy is of great interest.

The present study demonstrated that the AHNAK protein and mRNA expressions were all upregulated in decidua, decidual immune cells (DICs), and PBMCs of the patients with RPL when compared to the healthy controls (HCs). Furthermore, the level of *AHNAK* mRNA in PBMCs exhibited a potential value for RPL diagnosis, with an area under the curve (AUC) of 0.742. We also noted that the ratios of both decidual and blood AHNAK+CD4+ T cells in the population of CD4+ T cells were increased in patients with RPL; and, we hypothesized that AHNAK might affect IL-6 production by using a si-AHNAK treatment Jurkat T-cell line model. We proceeded to validate this observation using clinical specimens, and we discovered that the AHNAK+CD4+ T cells produced a significantly higher amount of IL-6 than the corresponding AHNAK-CD4+ T cells subpopulation. Besides, the ratios of both decidual and blood CD4+IL6+ T cells in the population of CD4+ T cells were also significantly higher in the RPL group than that in the fertile control, and the expression (%) of AHNAK was positively correlated with the expression (%) of IL-6 in CD4+ T cells. Together, our study uncovered an unanticipated role of AHNAK in RPL, suggesting that disorder of the maternal AHNAK-IL6 pathway in CD4+ T cells may contribute to RPL.

Methods

Reagents
Antibodies and fluorescent dyes are listed in Supplementary Table S1.

Human participants
Fresh decidua and peripheral venous blood specimens were obtained from patients with RPL and age//body mass index (BMI)-matched HCs at the obstetrics and gynecology department of the West China Second Hospital, between September 2021 and January 2022. Termination of all pregnancies occurred at 7–12 weeks' gestation; the pregnancies in the HC group were voluntarily terminated. RPL is defined as two or more consecutive failed pregnancies before 20–24 weeks, including embryonic and fetal losses [1], and in this study, the inclusion criteria for the above seven patients with RPL were (1) a history of at least two spontaneous abortions without defined etiology following a thorough clinical evaluation and laboratory testing, including normal parental chromosomes, a normal uterine structural study and endometrial biopsy, negative cervical cultures, and negative anti-phospholipid antibodies; (2) no history of a recent infection, hormonal therapy, or autoimmunity; (3) no history of smoking, drinking, or depression and (4) induction of abortion within 1 week of the fetal heartbeat ceasing. The fresh decidual materials were collected after the pregnancy termination operation without any medical pre-treatment and were acquired by dilatation and uterine curettage. Peripheral blood samples were collected at the same time (HC group, *N* = 7; RPL group, *N* = 7). These 14 subjects provided informed consent for the collections of decidua tissues and peripheral venous blood specimens for flow cytometry assays. The protocol for specimen collection was approved by the Medical Ethics Committee of West China Second Hospital of Sichuan University [Record number: 2020 (029)]. The 43 blood samples used for quantitative real-time polymerase chain reaction (qPCR) assays in this study (HC group, *N* = 17; RPL group, *N* = 26) were the EDTA anticoagulant blood samples remaining after the clinical laboratory completed the blood routine test (1–1.5 ml per sample).

Isolation of DICs and PBMCs
To isolate DICs, decidua was firstly rinsed with phosphate-buffered saline (PBS), then minced and digested with 1 mg/ml collagenase type IV (Sigma, USA) and 150 U/ml DNase I (Applichem, Germany) with gentle shaking for 45 min at 37°C. The released cells were resuspended with RPMI 1640 media (HyClone, USA) containing 10% fetal bovine serum (FBS) and filtered through 70 and 40 µm cell strainers (BD, USA). Next, we prepared 20%, 40%, and 60% (vol/vol) Percoll gradients by diluting the Percoll at a density of 1.130 g/ml (GE Healthcare, Sweden). The filtrate was layered on Percoll for density gradient centrifugation (600 g for 20 min). The DICs were collected from the 40%–60% layer of the gradient and washed with PBS. To isolate PBMCs, a 3 ml fresh blood sample from each participant was collected in a heparin anti-coagulated vacutainer tube (BD, USA) for flow cytometry analysis, and 1–1.5 ml of the remaining blood samples were collected in ethylenediaminetetraacetic acid (EDTA)-coagulated vacutainer tubes (BD, USA) for qPCR analysis. After dilution with PBS, the blood (Blood: Ficoll = 1:1) was carefully added to the Ficoll layer (TBD Science, Tianjin, China) and centrifuged at 450 g for 20 min with the brake off. The mononuclear layer was obtained and washed with PBS for subsequent analysis or stocked in the FBS containing 10% DMSO and 5% Dextran at –80°C until further study.

RNA sequencing and qPCR
The total RNA of the DICs and PBMCs were extracted using TRIzol reagent (Invitrogen, USA) according to the manufacturer's instructions. The RNA concentration and purity were measured using the NanoDrop ND-2000. Ribosomal RNA removal, cDNA library construction, and high-throughput sequencing using the Illumina HiSeq PE150 were conducted by Novogene Bioinformatics Technology (Beijing, China). Differential expression analysis was performed using the edgeR package in R. Genes with adjusted

P-value < 0.05 and |log2(FoldChange)| > 1 were considered differentially expressed genes (DEGs). GOseq and KOBAS (2.0) were used for GO and KEGG enrichment analyses, respectively. For qPCR, 500 ng of total RNA was converted to complementary DNA (cDNA) using an Evo M-MLV RT kit with gDNA cleaned for qPCR II Kit (AG111728, Accurate Biotechnology, Hunan, China) in a volume of 20 µl. The protocol for the qPCR experiment was as follows: 2 µl of RT product was used as a template, 0.4 µl of forward primer (10 µM), and 0.4 µl of reverse primer (10 µM) were added to 2 × SYBR®Green Pro Taq HS Premix (Lot, AG11701, Accurate Biotechnology, Hunan, China), for a total volume of 20 µl. Next, the following thermal cycle was used for the mixture: 95°C for 30 s and 40 cycles at 95°C for 5 s, and 60°C for 30 s using a qTOWER3G Analytik system (Jena, Germany). *GAPDH* served as the internal control. Primer sequences are listed in Supplementary Table S2.

Immunohistochemistry and immunofluorescence

All decidual sections for immunohistochemistry (IHC) assays were collected from the tissue bank of our Lab (HC group, N = 10; RPL group, N = 9). IHC assays were conducted by Servicebio Company (Wuhan, China), and the tissue sections were scanned by a Pannoramic MIDI scanner (Hungary) and quantified by ImageJ (National Institutes of Health, United States). The 1:100 diluted rabbit anti-human AHNAK antibody (SC247493, ProteinTech, Wuhan, China), and the 1:200 diluted HRP-conjugated rabbit anti-goat IgG secondary antibody (GB23303, Servicebio, Wuhan, China) were used for the IHC assays. An immunofluorescence assay of the Jurkat cell smears was carried out by the Biossci Company (Wuhan, China). The 1:50 diluted rabbit anti-human CD4 antibody (ab133616, Abcam, USA), the 1:100 diluted mouse anti-human AHNAK (ab68556, Abcam, USA), and the 1:400 diluted donkey anti-rabbit/mouse secondary antibodies (Life Technologies, USA) were used for the immunofluorescence assays.

Cell culture

The human Jurkat cell line was purchased from the Shanghai Institutes of Biological Sciences, Chinese Academy of Sciences (Shanghai, China). Cells were cultured in the RPMI 1640 medium (HyClone, USA) with 10% FBS (Biological Industries, Israel) in 5% CO_2 at 37°C according to the instructions. Human Jurkat T cells were used to elucidate the biological functions of CD4+ T cells.

Transfection assay

The human AHNAK siRNA oligonucleotide and control siRNA (5′-FAM-labelled) were purchased from the RiboBio Company (Guangzhou, China). Jurkat cells were seeded in 6-well plates and transfected at 100 nM siRNA concentration using the RiboFECT CP Transfection Kit (Ribobio, Guangzhou, China), followed by validations of mRNA and protein changes after 48 h transfection using qPCR and Western blotting, respectively.

Western blot analysis

Transfected Jurkat cells were lysed in RIPA buffer (Beyotime, Shanghai, China) containing protease inhibitor (Beyotime, Shanghai, China). Protein concentrations were detected by a BCA Protein Assay Kit (Beyotime, Shanghai, China).

Extracted proteins were separated by BeyoGel™ sodium dodecyl sulfate-polyacrylamide gel electrophoresis (SDS–PAGE) (Beyotime, Shanghai, China) and transferred to polyvinylidene fluoride (PVDF) membranes (Millipore, USA). The membranes were blocked in QuickBlock™ Western (Beyotime, Shanghai, China) followed by overnight incubation with the mouse anti-human AHNAK at a dilution of 1:500 (ab68556, Abcam, USA) and the mouse anti-human GAPDH at a dilution of 1:10 000 (60004-1-lg, ProteinTech, Wuhan, China), respectively. After washing three times, the membranes were incubated with the secondary antibody at a dilution of 1:5000 (ZB-2305, ZSGB-BIO, Beijing, China). The signals were detected using the Chemidoc imaging system (Bio-Rad, USA).

Flow cytometry

Firstly, live/dead cell discrimination was performed using the Zombie Aqua Fixable Viability Kit (BioLegend, USA). Approximately 1×10^6 cells were then resuspended in 100 µl of 3% FBS/PBS solution. For surface staining, cells were stained with anti-human CD45, CD3, and CD4 for 20 min in the dark at room temperature (RT) after 10 min of incubation with Fc-Block (BioLegend, USA). For intracellular AHNAK staining, cells were fixed and permeabilized using the eBioscience™ Fixation Permeabilization kit (Invitrogen, USA). Subsequently, the cells were incubated with 0.2 µg of primary rabbit anti-AHNAK (16637-1-AP, ProteinTech, Wuhan, China) in 100 µl of cell suspension for 30 min in the dark at RT. Next, we washed the cells with 1 ml 1× permeabilization buffer (Invitrogen, USA), and the cells were again incubated with 100 µl of fluorochrome-conjugated secondary antibody (1:2500) dilution (Alexa Fluor 488-conjugated AffiniPure goat anti-rabbit IgG (H+L), Servicebio, Wuhan, China). For intracellular cytokine IL-6 staining, cells were stimulated with a lipopolysaccharide (LPS) solution (1 µg/ml) for 4 h, and the addition of protein transport inhibitors, including brefeldin A (BioLegend, USA) and monensin (BioLegend, USA) was critical. Flow cytometry data acquisition was performed using a FACS Celesta flow cytometer (BD, USA), and analyzed using the FlowJo software V.10. All flow cytometry data was compensated in the FlowJo software V.10 by using single stained controls.

Enzyme-linked immunoassay (ELISA)

The IL-6 concentrations in the supernatants of transfected Jurkat cells were examined with an ELISA Kit (SEKH-0013, Solarbio, Beijing, China) according to the manufacturer's instructions.

Statistical analysis

The comparative cycle threshold method ($2^{-\triangle\triangle CT}$) was used to measure dynamic changes in specifically selected mRNA levels in qPCR analyses. The receiver operating characteristic (ROC) curve was applied for the evaluation of diagnostic performance. Student's t-test, Mann–Whitney test, or paired t-test were carried out to compare the differences between groups. Pearson correlation was used for the correlation analysis. Differences were considered significant when the P-value < 0.05.

Results

Patients with RPL exhibited an altered transcriptome in DICs

To better understand the pathogenetic mechanism of RPL, we performed RNA-seq to investigate the DEGs in DICs between the RPL group and the HC group. Here three healthy DIC samples and three RPL DIC samples were used for RNA-seq analysis (Table 1). Although two outlier samples were identified by principal component analysis (PCA), our sequence data still revealed 407 genes that were differentially expressed between the two groups (DEGs were defined as adjusted P-value < 0.05 and |log2(FoldChange)| > 1). Among which, 210 genes were upregulated, and 197 genes were downregulated. The DEGs were visualized using a heatmap and a volcano plot (Fig. 1A and B). The PCA distribution 3D plot is exhibited in Fig. 1C.

GO and KEGG pathway analyses

To acquire better knowledge about the biological functions of these DEGs, gene ontology (GO) analysis was applied to classify their cellular, biological, and molecular functions. The results are shown in Fig. 1D–F. GO analysis identified numerous functional pathways that were associated with coagulation, including platelet degranulation, hemostasis, and blood coagulation. Consistent with the earlier research data, the activation of platelets at the maternal-fetal interface affected trophoblast behavior, which has been implicated in severe pregnancy pathologies [21]. The KEGG pathway analysis clearly revealed that the DEGs were associated with immune-related diseases, such as toxoplasmosis, systemic lupus erythematosus, and rheumatoid arthritis. Pathways related to immune regulation were also significantly enriched, including complement and coagulation cascades, antigen processing, and presentation and allograft rejection (Fig. 1G). Collectively, these results suggested that pregnancy is a common immunization event and immune system disorders may be associated with RPL.

Network construction of immune-related DEGs

Based on the above results of pathway enrichment, we next focused on the DEGs with the potential to participate in the immunological mechanisms of RPL. We downloaded the immune gene list from the IMMPORT database (https://www.immport.org/home). The Venn diagram (Fig. 2A) exhibited the intersection between the DEGs obtained from our RNA-seq results and the immune genes downloaded from the IMMPORT database. The pool of 407 DEGs and 1795 immune genes shared (intersection) a total of 21 genes, including 11 upregulated genes and 10 downregulated genes (Table 2). A protein–protein interaction (PPI) network based on 21 immune-related DEGs was constructed by the STRING database (https://string-db.org) (Fig. 2B).

qPCR validation of immune-related DEGs

Next, based on the fold change values from the RNA-seq data, we conducted qPCR to validate the mRNA expression levels of the most significantly upregulated and downregulated immune-related DEGs using the clinical specimens (including *VAV1*, *VAV3*, *NEO1*, and *LTBP4*). In addition, another two genes, *AHNAK* [22] and *BLNK* [23], which were reported to be associated with pregnancy complications, were also enrolled in our validation cohort (Table 2). As shown in Fig. 2C, the mRNA expression levels of *AHNAK, VAV1,* and *VAV3* were significantly higher in the RPL group than those in the HC group, which were consistent with our RNA-seq results. Although *NEO1*, *LTBP4*, and *BLNK* also presented significant changes, their qPCR results contradicted our RNA-seq results. Therefore, we focused more on the expressions of AHNAK, VAV1, and VAV3. We observed that the AHNAK protein was highly expressed in female tissues, including the cervix and uterus; however, VAV1 and VAV3 proteins were expressed at low levels in female tissues according to data from the HPA database (https://www.proteinatlas.org) (Supplementary Fig. S1). Combining the results mentioned above, we chose the more highly expressed AHNAK for the subsequent analyses.

AHNAK was upregulated in patients with RPL

In the next step, we examined the protein expression of AHNAK in the decidua of patients with RPL and HCs using IHC. Our results showed that AHNAK protein was more highly expressed in the decidua of patients with RPL than that in the HCs' decidual tissues (Fig. 3A). We further detected the expression of *AHNAK* mRNA in the PBMCs from 26 patients with RPL and 17 HCs using qPCR. It was found that *AHNAK* in the PBMCs showed significant up-regulation in the RPL group (Fig. 3B), which was in line with our findings of RNA-seq for DICs above. Moreover, we have also performed a subgroup analysis by age, which demonstrated that patients with RPL who were older than age 35 years expressed *AHNAK* at higher levels than those who were age 35 years or younger. (Fig. 3C). Based on the distinct *AHNAK* mRNA expression between

Table 1 : Information for the specimens used for RNA sequencing.

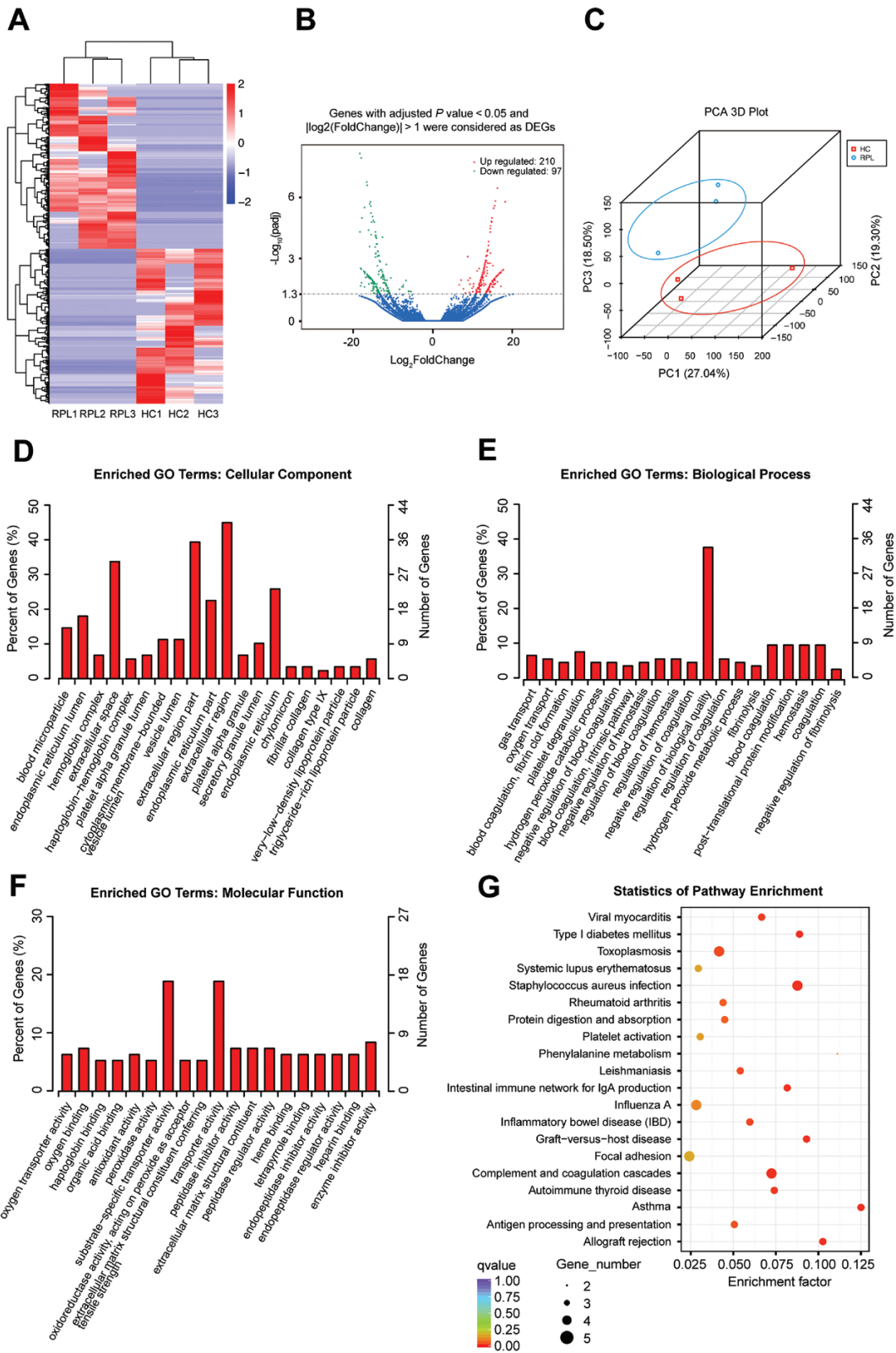| Patients	Maternal age (year)	BMI (kg/m^2)	Gestational age (week)	No. of prior miscarriages (N)
HC-1	33	22.5	8	0
HC-2	33	21.7	9	0
HC-3	29	23.4	9	0
RPL-1	31	23.1	9	2
RPL-2	34	23.7	10	2
RPL-3	34	20.6	10	2

Figure 1: Transcriptome changes of DICs isolated from patients with RPL. (A) Heatmap of the *z*-scores for 407 DEGs identified using RNA-seq showed that genes distinguished the RPL samples from the HC samples. (B) Volcano plot of DEGs with an adjusted *P*-value < 0.05 and more than 2-fold change. (C) The PCA distribution 3D plot of our RNA-seq. (D–F) GO analysis of the DEGs upon RPL using GOseq. (G) The top 20 significantly enriched KEGG pathways of DEGs. DICs, decidual immune cells; HCs, healthy controls; RPL, recurrent pregnancy loss; DEGs, differentially expressed genes. GO, gene ontology.
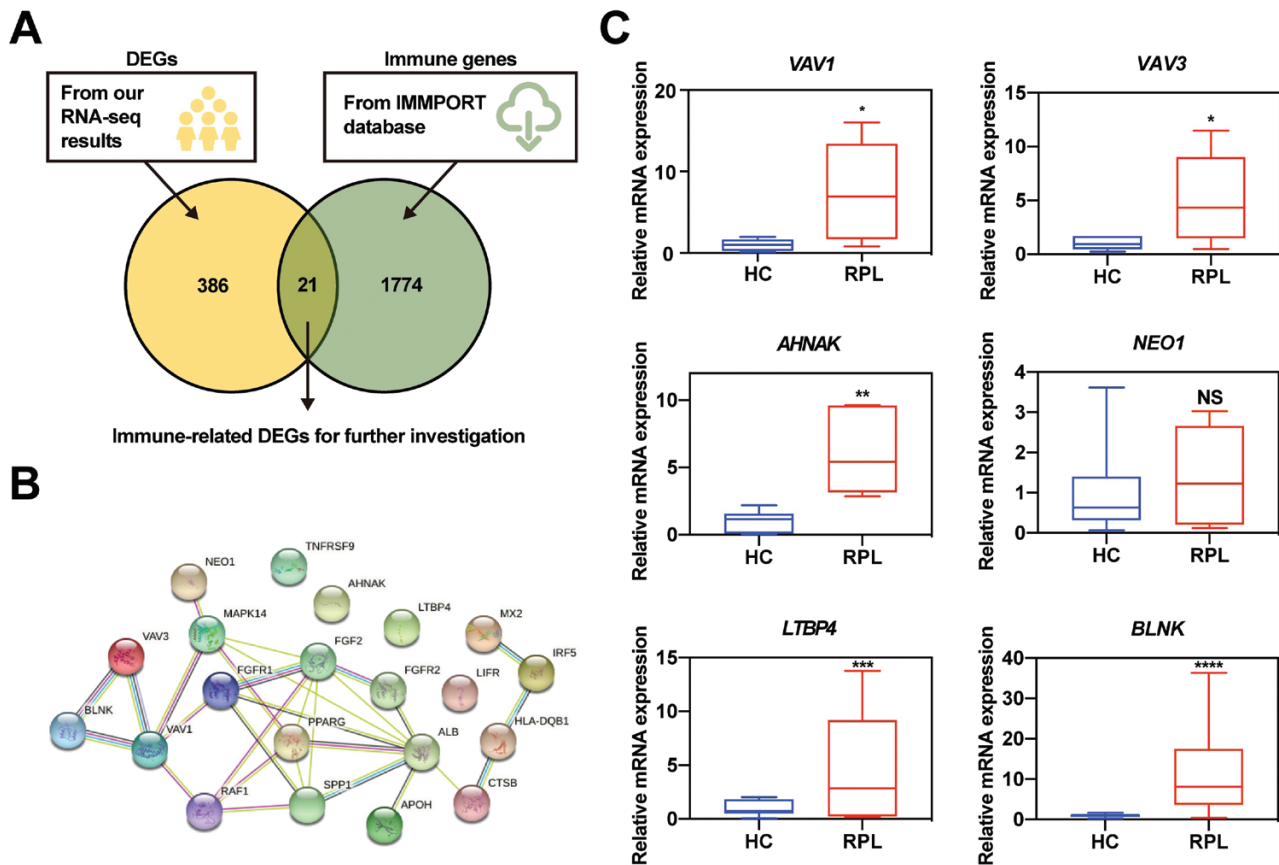
Figure 2: Network of immune-related DEGs. (A) Venn diagram showing 21 overlapping elements between DEGs obtained from our RNA-seq data and immune genes loaded from the IMMPORT database. (B) Construction of the PPI network of the 21 immune-related DEGs using the STRING database. (C) *VAV1*, *VAV3*, *AHNAK*, *NEO1*, *LTBP4*, and *BLNK* mRNA levels were validated in clinical DIC samples. HC group, $N = 7$; RPL group, $N = 7$. *$P < 0.05$, **$P < 0.01$, ***$P < 0.001$, ****$P < 0.0001$. DEGs, differentially expressed genes; PPI, protein–protein interaction; DICs, decidual immune cells; HCs, healthy controls; RPL, recurrent pregnancy loss.

Table 2 : Immune-related DEGs

Gene	Fold change	*P* value	*P* adjust value
Upregulated			
VAV1	17.78	2.78E–06	0.003
VAV3	16.82	5.24E–06	0.005
SPP1	15.54	4.13E–05	0.017
HLA-DQB1	14.98	6.08E–05	0.022
PPARG	14.21	5.73E–05	0.021
AHNAK	13.40	0.0002	0.045
MX2	12.15	2.02E–05	0.011
FGFR1	11.74	3.90E–05	0.017
LIFR	11.69	9.46E–05	0.030
CTSB	11.68	2.40E–06	0.003
TNFRSF9	11.33	8.56E–05	0.028
Downregulated			
NEO1	–17.99	3.84E–13	1.29E–08
LTBP4	–17.20	6.15E–05	0.023
ALB	–16.19	9.79E–09	4.02E–05
FGFR2	–14.13	0.0001	0.035
BLNK	–13.98	6.58E–08	0.0001
MAPK14	–13.25	8.47E–07	0.001
APOH	–12.27	2.94E–05	0.014
IRF5	–12.22	3.00E–05	0.014
FGF2	–7.45	4.56E–05	0.018
RAF1	–5.86	0.0001	0.037

the two groups, we next evaluated whether *AHNAK* in PBMCs may serve as a potential diagnostic marker for RPL. Of interest, the receiver operating characteristic (ROC) curve for the blood *AHNAK* classifier exhibited a good AUC (AUC, 0.742; 95% CI, 0.587–0.897; *P*-value = 0.008) (Fig. 3D). Together, the upregulation of AHNAK protein and mRNA expressions occurred in RPL, showing it might act as a potential diagnostic marker for RPL.

The frequencies of decidual and blood AHNAK+CD4+T cells were increased in patients with RPL

Dysregulation of CD4+ Th cell subset immunity during pregnancy has been reported to induce obstetrical complications, including RPL [24]. Previous research has demonstrated that AHNAK was especially required for calcium signaling during CD4+ T-cell activation [12, 13]. Therefore, we further focused on the potential effect of AHNAK on CD4+ T cells in RPL pathologies. The cell (Live CD45+CD3+CD4+AHNAK+) gating strategy and representative scatter plots are presented in Fig. 4A. Our results demonstrated that the percentages of decidual and blood CD4+ AHNAK+ T cells in the CD4+ T cell population were both higher in the RPL group than those in the HC group (Fig. 4B and C). Hence, we hypothesized that the elevated AHNAK in CD4+ T cells may provoke its dysfunction, leading to the RPL phenotype.
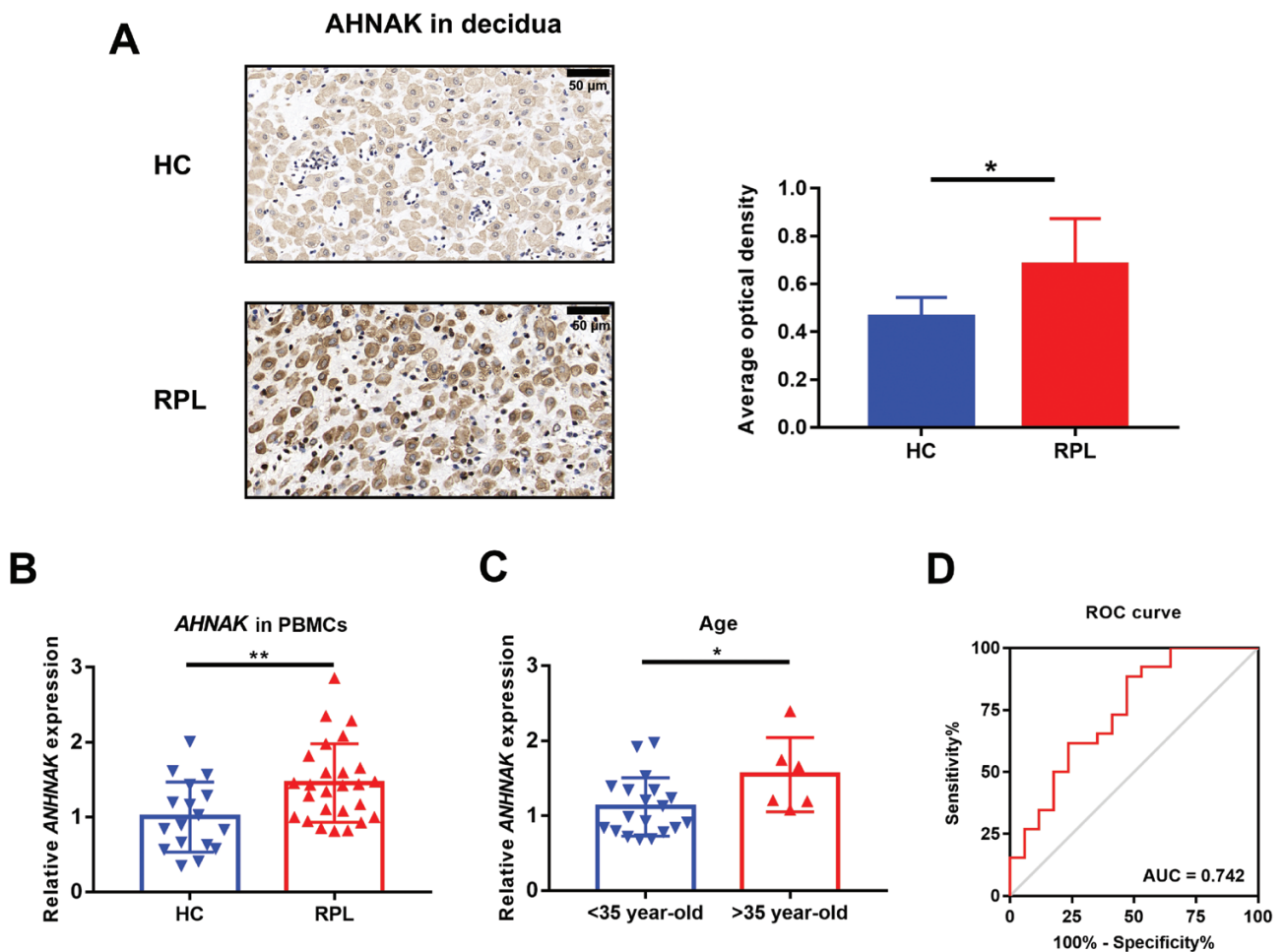
Figure 3: AHNAK was upregulated in patients with RPL. (A) Representative IHC staining results for the expressions of AHNAK proteins in the decidual tissues. Scale bar, 50 μm. (B) *AHNAK* mRNA levels in PBMCs were elevated in patients with RPL when compared to that in the HCs. (C) Patients with RPL who were older than age 35 years expressed *AHNAK* at higher levels than those who were age 35 years or younger. (D) ROC curve of *AHNAK* mRNA in PBMCs for discriminating patients with RPL from HCs, and the AUC was 0.742. HC group, $N = 10$; RPL group, $N = 9$ for IHC. HC group, $N = 17$; RPL group, $N = 26$ for qPCR. *$P < 0.05$, **$P < 0.01$. HCs, healthy controls; RPL, recurrent pregnancy loss. ROC, receiver operating characteristic; AUC, area under the curve.

Elevated AHNAK in CD4+ T-cells displayed the feature of producing more IL-6

The CD4+ Jurkat T cell line has been frequently and successfully used for T-cell research, and the AHNAK was localized in its cytosol (Fig. 5A). To assess the effect of AHNAK on CD4+ T cells, AHNAK siRNA was used to treat the Jurkat T cell line *in vitro*, and the mRNA and protein levels of AHNAK were determined by qPCR and Western blotting after transfection, respectively (Fig. 5B–D). Next, we investigated the mRNA expressions of Th1 cytokines (TNF-α and IFN-γ) and Th2 cytokines (IL-13, IL-5, IL-4, and IL-6) in Jurkat cells with and without AHNAK siRNA treatment (Fig. 5E). The cytokine with the most pronounced change after AHNAK siRNA transfection was the IL-6, and the decreased IL-6 productions in the AHNAK siRNA transfected Jurkat cells were also confirmed by flow cytometry and ELISA assays (Fig. 5F–G). IL-6 has been implicated as a multifunctional cytokine during pregnancy; however, the role of IL-6 in RPL remains controversial. We observed that in almost all our decidua and blood samples of HCs, RPL, or all participates, the AHNAK+CD4+ T cells produced a significantly higher amount of IL-6 than the corresponding AHNAK-CD4+ T-cells subpopulation (Fig. 6A and B). Moreover, in both decidual and blood CD4+ T-cell populations, the ratios of IL-6+CD4+ T cells were also higher in patients with RPL than those in HCs and positively correlated with the ratios of AHNAK+CD4+ T cells (Fig. 6C–F). Overall, these findings demonstrated that the elevated AHNAK in CD4+ T cells may promote IL-6 production, which leads to the disruption of immune balance at maternal–fetal interface of patients with RPL.

Discussion

Chromosomal anomalies, uterine anatomic defects, endocrinological problems, autoimmune disease, and others may form the category of so-called "explained" reasons for RPL; immune dysregulation may also account for a proportion of the "unexplained' cases of RPL [20]. Clinicians should be alert to an immune disorder-mediated miscarriage that might contribute to a definitive diagnosis. In addition, the elucidation of the immune regulation mechanism in RPL can contribute to the development of new drugs and clinical treatments and some immune-related biomarkers are useful to improve diagnosis, clinical predictive capability, and novel therapeutic efficacy of RPL.
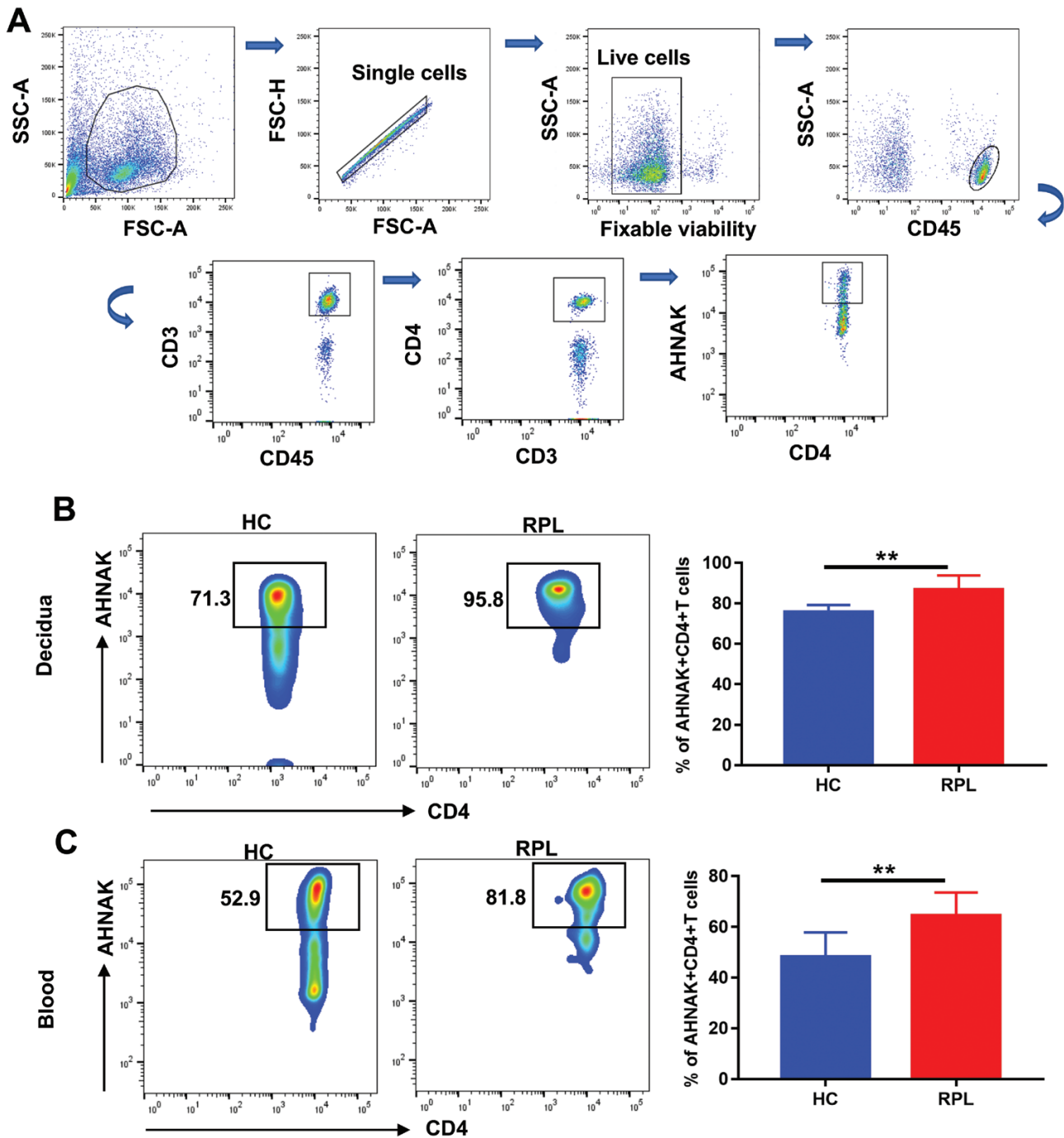
Figure 4: Patients with RPL exhibited enhanced ratios of decidual and blood AHNAK+CD4+ T cells. (A) The gating strategy of flow cytometry data. (B–C) Representative image showing the ratios of decidual and blood AHNAK+CD4+ T cells in the CD4+ T cell population were increased in the RPL group. HC group, $N = 7$; RPL group, $N = 7$. *$P < 0.05$, **$P < 0.01$. HC, healthy control; RPL, recurrent pregnancy loss.

AHNAK is a large protein orchestrating a range of diverse biological processes and chemotherapeutic responses [25]. Several studies have shown that the dysregulated levels of AHNAK are linked with numerous cancers, such as breast cancer, gastric cancer, and ovarian cancer [7, 26, 27]. In addition, overexpression of AHNAK could influence the proliferation, migration, and apoptosis of HTR-8/SVneo cells [22]. Our present study was designed to confirm the immunomodulatory effects of AHNAK in RPL. The flow diagram of this work is shown in Fig. 7. We first observed that patients with RPL exhibited an altered transcriptome in DICs. Then, based on the validation results of RNA-seq data, we identified that the protein and mRNA levels of AHNAK were all upregulated in the decidua, DICs, and PBMCs of patients with RPL when compared to that in the HCs. In addition, *AHNAK* in the PBMCs was indicated to be valuable in the diagnosis of RPL with a high AUC (0.742). As previously reported, certain genes and miRNAs in PBMCs or immune cells have been considered to be diagnostic or predictive biomarkers for immune-related diseases [28, 29]. Compared to serum biomarkers, whether biomarkers in PBMCs have advantages in the diagnosis of immune-related conditions requires further investigation.
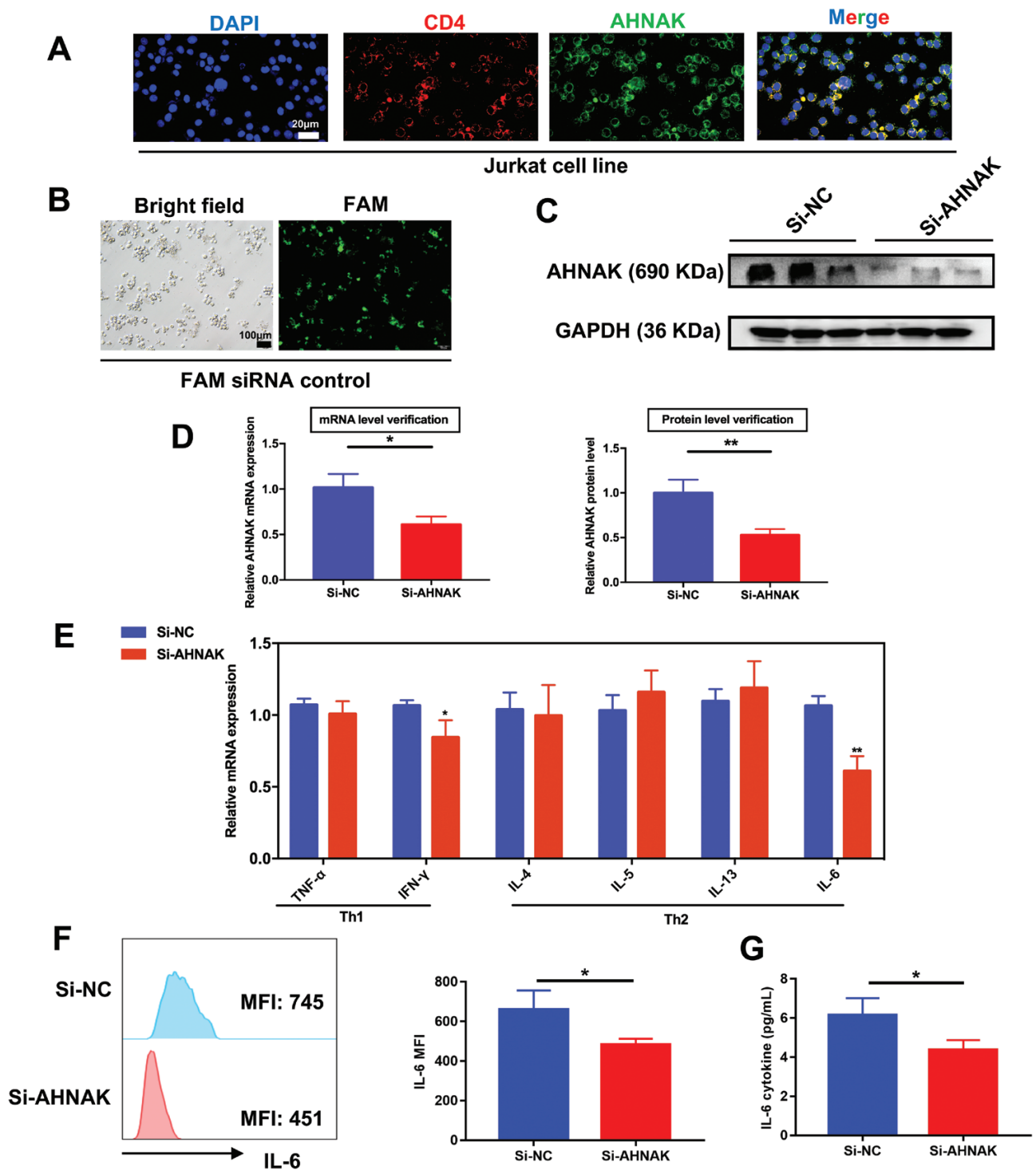
Figure 5: The effect of AHNAK on cytokine production in the Jurkat cell line. (A) AHNAK was localized in the cytosol of the CD4+ Jurkat T-cell line. Scale bar, 20 μm. (B) Representative image of Jurkat cells after transfection with the FAM-siRNA control. Scale bar, 100 μm. (C–D) The mRNA and protein levels of AHNAK after siRNA control (Si-NC) and siRNA AHNAK (Si-AHNAK) transfection were determined by qPCR and western blotting, respectively. (E) The mRNA expressions of classical Th1 type cytokines and Th2 type cytokines in the transfected Jurkat cell line. (F) The MFI of IL-6 in the transfected Jurkat cells was detected using the flow cytometry assay. (G) The concentration of IL-6 in the supernatant of transfected Jurkat cells was detected using the ELISA assay *$P < 0.05$, **$P < 0.01$. MFI, mean fluorescence intensity.

Human CD4+ T cells can be classified into Th1, Th2, regulatory T (Treg), and Th17 cells based on their pattern of cytokine production, and they display different biological functions [30, 31]. Research has proposed that successful pregnancy is a Th2 type phenomenon, and Th1 type reactivity is harmful to pregnancy [20]. The dysregulation of Th cell immunity has been confirmed to be present in RPL [24]. In another respect, previous studies have reported that AHNAK is highly expressed by CD4+ T cells and acts as a critical component for calcium signaling [12]. Data from the AHNAK-KO
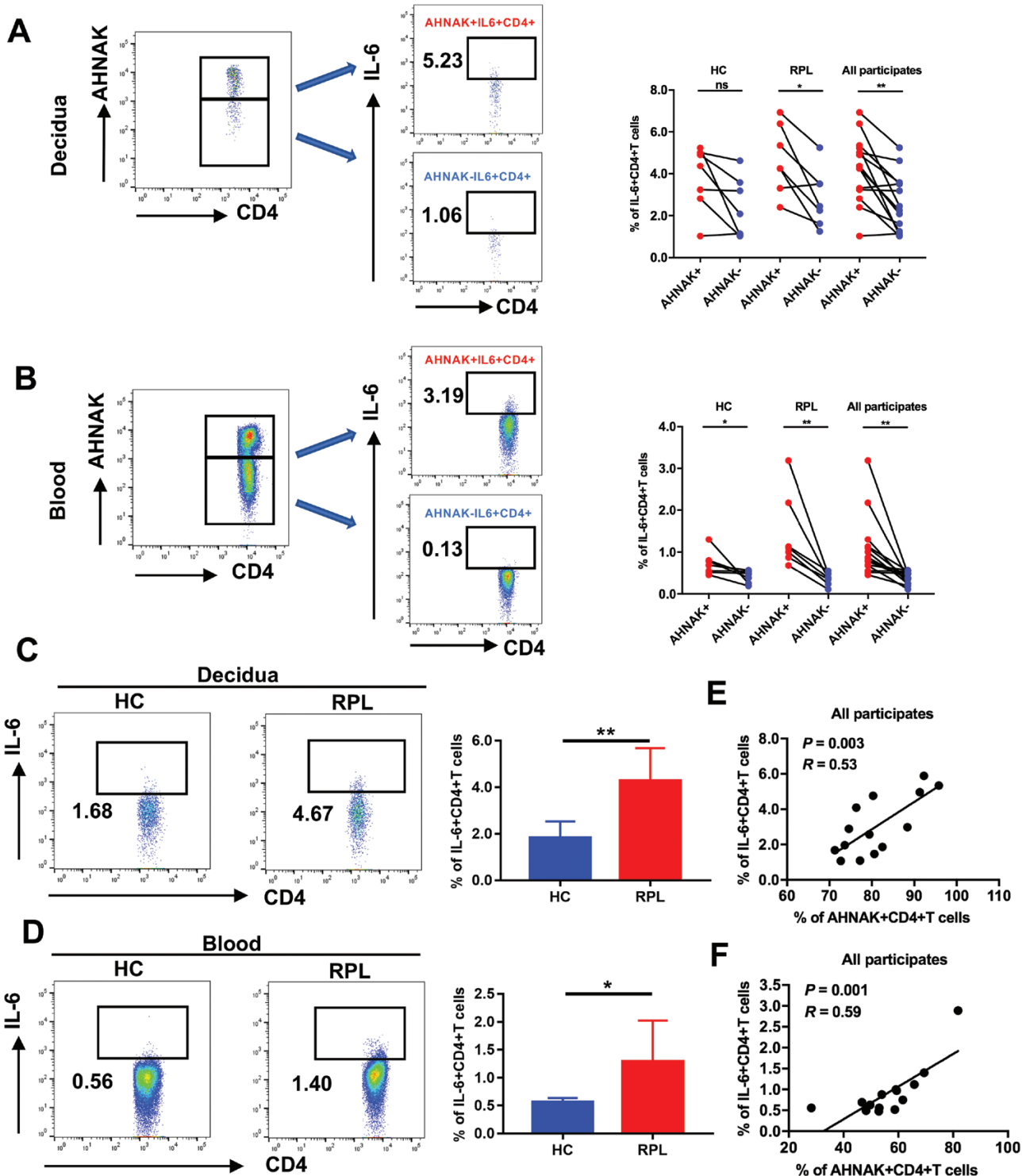
Figure 6: Impact of AHNAK on IL-6 production in human CD4+ T cells (A–B) The frequencies of decidual and blood IL-6 expression (%) in AHNAK+ and AHNAK– CD4+ T cells. (C–D) Representative images showing the frequencies of decidual and blood IL-6+CD4+ T cells in the RPL and HC groups. (E–F) Pearson's correlation between expressions (%) of decidual (E) and blood (F) AHNAK and IL-6 in human CD4+ T cells. HC group, $N = 7$; RPL group, $N = 7$; all participates, $N = 14$. *$P < 0.05$, **$P < 0.01$. HCs, healthy controls; RPL, recurrent pregnancy loss.

mice suggests that AHNAK deficiency could result in CD4+ T cell inactivation and impairment of Th1 and Th2 immunity [13]. In addition, a novel protein, Mus musculus Gm40600, could promote CD4+ T cell activation by interacting with AHNAK [32]. Collectively, AHNAK is important for the activation and immune function of CD4+ T cells. In this study,

we identified that both decidual and blood CD4+ T cells expressed higher constitutive levels of AHNAK (%) in patients with RPL than that in HCs. Thus, we guessed that CD4+ T cells may be regulated by elevated AHNAK, presenting more active phenomena in patients with RPL and exhibiting altered Th1 and Th2 cytokine production.
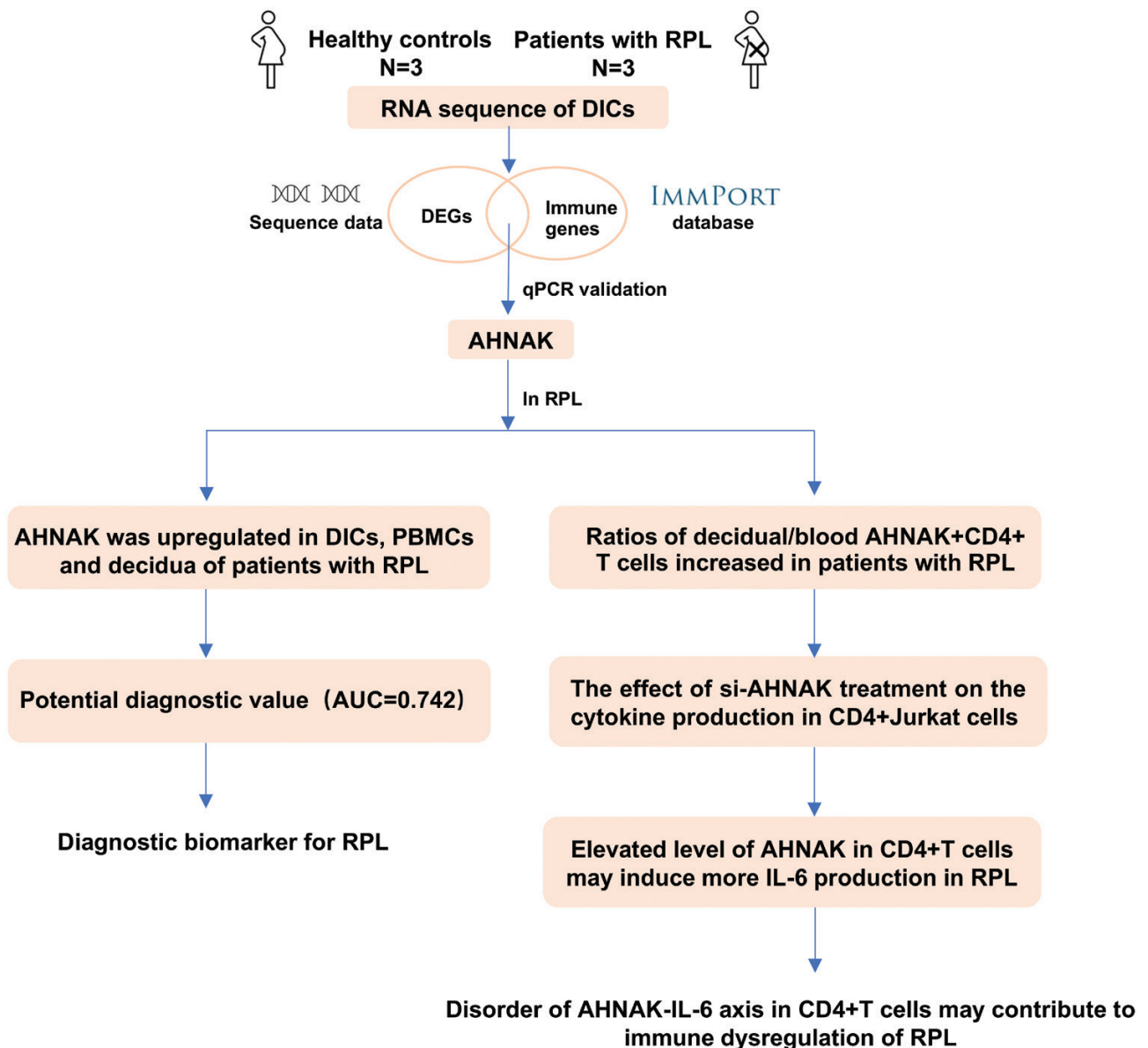
Figure 7: The flow diagram of the current work. AHNAK may act as a diagnostic marker for RPL, and the disorder of AHNAK-IL6 axis in CD4+ T cells may contribute to the immune dysregulation of RPL.

To further explore the effect of AHNAK on CD4+ T cells, we used a well-established cell line, the CD4+ Jurkat T cell line, which has been frequently used for T cell studies since the cell line is easy to access, grow and transfect [33, 34], to validate the relationship between AHNAK and classical Th1/2 cytokine secretion. We discovered that Jurkat T-cells treated with AHNAK siRNA exhibited a significantly decreased IL-6 mRNA level. This finding was further confirmed at the protein level by flow cytometry and ELISA assays. We then proceeded to validate this observation using clinical specimens. The results showed that the frequencies of decidual and blood CD4+ T cells simultaneously producing IL-6 were much higher in the AHNAK+ compartment compared to the AHNAK-one. Moreover, in both RPL patients' decidua and blood samples, the ratios of IL-6+CD4+ T cells in the population of CD4+ T cells were higher than that in HCs and positively correlated with the ratios of AHNAK+CD4+ T cells. Together, our results demonstrated

that the elevated AHNAK+CD4+ T cells in RPL could produce more IL-6, which may have an impact on the immune balance at the maternal–fetal interface. Earlier studies have reported that the concentration of IL-6 was significantly lower in the supernatants of cultured PBMCs from patients with RPL [20], which seemed to contradict our discovery. However, growing evidence has highlighted that an increased IL-6 level could lead to the transformation of CD4+ T cells into Th17 cells, resulting in the Treg/Th17 imbalance [35]. Of note, the balance of Th17 and Treg cells has been reported to be important for successful pregnancy [36], and the increase in Th17 type cells [24, 37] and the depletion of Treg cells [38, 39] are associated with RPL. Hence, we suspected that the elevated levels of AHNAK (%) in CD4+ T cells led to the increased secretion of IL-6, which contributed to the imbalanced Treg/Th17 ratio and finally resulted in early pregnancy loss. Additional studies are clearly required to delineate these mechanisms further.

However, the above data presented here may be viewed with two caveats. First, embryo aneuploidy is responsible for a major cause of spontaneous abortions [40], while no such detailed clinical information (such as chromosomal microarray or karyotyping) was collected for our blood samples for the qPCR experiments (HC $n = 17$ and RPL $n = 26$). Thus, it was not possible to rule out the possibility of chromosomal abnormalities in these 26 patients with RPL or aneuploidy in the fetuses. Hence, a more rigorous study on blood samples of patients with RPL is needed to confirm whether AHNAK can potentially serve as a diagnostic or correlative biomarker. Second, our current study, like many of the studies on human recurrent pregnancy loss, has still not demonstrated a direct cause-and-effect relationship between the inflammatory event and pregnancy loss; for instance, an inflammatory maternal response to a fetus that has died due to non-immunological factors, could well manifest the IL-6 secretion in CD4+ T cells and/or the production of other inflammatory cytokines at the maternal–fetal interface. However, given the association between IL-6 dysregulation and pregnancy failure, and the previously demonstrated deleterious effects of IL-6 on the conceptus and the fetal [41, 42], it is suggested that IL-6-mediated effects may have been the cause of pregnancy failure in at least a proportion of the cases. Additional studies will be needed to confirm causality and determine the mechanism of action.

We also acknowledge that several limitations are noted in the design of the current report. There were a rather low number of samples in each group for RNA-seq, and we found the heterogeneity within groups still remained high using PCA analysis. Thus, more clinical samples for RNA-seq are needed in the future to identify accurate biomarkers for RPL. All enrolled patients were from a Chinese hospital cohort, and the majority had the same background. In addition, only a small number of their samples were analyzed; therefore, our results must be interpreted with caution. The relationship between AHNAK and RPL in other ethnic/genetic backgrounds and a robust statistical validation from a larger number of specimens should be addressed. Moreover, although the Jurkat T-cell lines used in this study have been well characterized and widely used in previous studies [43, 44], they still differ from primary CD4+ T cells. It is possible that cell lines might contain unknown artifacts in characteristics and cell culture that affect their epigenetic profiles and regulatory function and future studies using primary cells and/or animal models will be helpful to confirm our findings in this report. We only showed that AHNAK affected IL-6 production in CD4+ T cells, however, whether si-AHNAK treatment in the Jurkat cell line has an effect on other classical cytokines production, such as IL-10, TGF-β, or IL-1β, remains to be explored. In addition to the effects on CD4+ T cells, whether AHNAK has effects on the proliferation and function of other immune cells at the maternal-fetal interface also warrants further investigation.

Supplementary data

Supplementary data is available at *Clinical and Experimental Immunology* online.

Acknowledgments

We would like to thank the outpatient operating room and obstetrics department of West China Second University Hospital for the clinical samples.

Conflict of interest

All authors declare no conflict of interest.

Author contributions

Liman Li performed the experiments and drafted the initial manuscript. Yuan Liu performed the qPCR assays and cell culture assays. Ting Feng performed the flow cytometry assays. Wenjie Zhou collected clinical samples. Hong Li and Yanyun Wang were liable for oversight and leadership responsibility for research activity planning and execution. All authors contributed to the article and approved the submitted version.

Ethics approval and consent to participate

The Medical Ethics Committee of West China Second Hospital of Sichuan University [Record number: 2020 (029)] has proved our study (approval number: 81971461). The patients/participants provided written informed consent to participate in this study.

Data Availability

All the raw sequence reads used in this study are available in the NCBI SRA database and can be accessed with BioProject ID PRJNA813430.

References

1. Dimitriadis E, Menkhorst E, Saito S, Kutteh WH, Brosens JJ. Recurrent pregnancy loss. *Nat Rev Dis Primers* 2020, 6, 98. doi:10.1038/s41572-020-00228-z.
2. Coomarasamy A, Dhillon-Smith RK, Papadopoulou A, Al-Memar M, Brewin J, Abrahams VM, et al. Recurrent miscarriage: evidence to accelerate action. *Lancet* 2021, 397, 1675–82. doi:10.1016/S0140-6736(21)00681-4.
3. Bagkou Dimakou D, Lissauer D, Tamblyn J, Coomarasamy A, Richter A. Understanding human immunity in idiopathic recurrent pregnancy loss. *Eur J Obstet Gynecol Reprod Biol* 2021, 270, 17–29.
4. Yockey LJ, Iwasaki A. Interferons and proinflammatory cytokines in pregnancy and fetal development. *Immunity* 2018, 49, 397–412. doi:10.1016/j.immuni.2018.07.017.
5. Li L, Feng T, Zhou W, Liu Y, Li H. miRNAs in decidual NK cells: regulators worthy of attention during pregnancy. *Reprod Biol Endocrinol* 2021, 19, 150. doi:10.1186/s12958-021-00812-2.
6. Gentil BJ, Delphin C, Mbele GO, Deloulme JC, Ferro M, Garin J, et al. The giant protein AHNAK is a specific target for the calcium- and zinc-binding S100B protein: potential implications for Ca^{2+} homeostasis regulation by S100B. *J Biol Chem* 2001, 276, 23253–61. doi:10.1074/jbc.M010655200.
7. Cai Y, Hu Y, Yu F, Tong W, Wang S, Sheng S, et al. AHNAK suppresses ovarian cancer progression through the Wnt/beta-catenin signaling pathway. *Aging (Albany NY)* 2021, 13, 23579–87. doi:10.18632/aging.203473.
8. Ye R, Liu D, Guan H, AiErken N, Fang Z, Shi Y, et al. AHNAK2 promotes thyroid carcinoma progression by activating the NF-kappaB pathway. *Life Sci* 2021, 286, 120032. doi:10.1016/j.lfs.2021.120032.

9. Guo L, Wu Q, Ma Z, Yuan M, Zhao S. Identification of immune-related genes that predict prognosis and risk of bladder cancer: bioinformatics analysis of TCGA database. *Aging (Albany NY)* 2021, 13, 19352–74. doi:10.18632/aging.203333.

10. Matza D, Badou A, Jha MK, Willinger T, Antov A, Sanjabi S, et al. Requirement for AHNAK1-mediated calcium signaling during T lymphocyte cytolysis. *Proc Natl Acad Sci USA* 2009, 106, 9785–90. doi:10.1073/pnas.0902844106.

11. Matza D, Flavell RA. Roles of Ca(v) channels and AHNAK1 in T cells: the beauty and the beast. *Immunol Rev* 2009, 231, 257–64. doi:10.1111/j.1600-065X.2009.00805.x.

12. Matza D, Badou A, Kobayashi KS, Goldsmith-Pestana K, Masuda Y, Komuro A, et al. A scaffold protein, AHNAK1, is required for calcium signaling during T cell activation. *Immunity* 2008, 28, 64–74. doi:10.1016/j.immuni.2007.11.020.

13. Choi EW, Lee HW, Lee JS, Kim IY, Shin JH, Seong JK. AHNAK-knockout mice show susceptibility to *Bartonella henselae* infection because of CD4+ T cell inactivation and decreased cytokine secretion. *BMB Rep* 2019, 52, 289–94.

14. Comba C, Bastu E, Dural O, Yasa C, Keskin G, Ozsurmeli M, et al. Role of inflammatory mediators in patients with recurrent pregnancy loss. *Fertil Steril* 2015, 104, 1467–74.e1. doi:10.1016/j.fertnstert.2015.08.011.

15. Begum A, Mishra A, Das CR, Das S, Dutta R, Kashyap N, et al. Impact of TNF-alpha profile in recurrent pregnancy loss pathogenesis: a patient based study from Assam. *J Reprod Immunol* 2021, 148, 103430. doi:10.1016/j.jri.2021.103430.

16. Kniotek M, Zych M, Roszczyk A, Szafarowska M, Jerzak MM. Decreased production of TNF-alpha and IL-6 inflammatory cytokines in non-pregnant idiopathic RPL women immunomodulatory effect of sildenafil citrate on the cellular response of idiopathic RPL women. *J Clin Med* 2021, 10, 3115.

17. Murakami M, Kamimura D, Hirano T. Pleiotropy and specificity: insights from the interleukin 6 family of cytokines. *Immunity* 2019, 50, 812–31. doi:10.1016/j.immuni.2019.03.027.

18. Mirabella F, Desiato G, Mancinelli S, Fossati G, Rasile M, Morini R, et al. Prenatal interleukin 6 elevation increases glutamatergic synapse density and disrupts hippocampal connectivity in offspring. *Immunity* 2021, 54, 2611–2631.e8. doi:10.1016/j.immuni.2021.10.006.

19. Zhang L, Lu B, Wang W, Miao S, Zhou S, Cheng X, et al. Alteration of serum neuregulin 4 and neuregulin 1 in gestational diabetes mellitus. *Ther Adv Endocrinol Metab* 2021, 12, 20420188211049614. doi:10.1177/20420188211049614.

20. Raghupathy R, Makhseed M, Azizieh F, Omu A, Gupta M, Farhat R. Cytokine production by maternal lymphocytes during normal human pregnancy and in unexplained recurrent spontaneous abortion. *Hum Reprod* 2000, 15, 713–8. doi:10.1093/humrep/15.3.713.

21. Forstner D, Maninger S, Nonn O, Guettler J, Moser G, Leitinger G, et al. Platelet-derived factors impair placental chorionic gonadotropin beta-subunit synthesis. *J Mol Med (Berl)* 2020, 98, 193–207. doi:10.1007/s00109-019-01866-x.

22. Dong X, Zhao J, Han J, Han XJ, Zhao CM, Zou AX, et al. MiR-222-5p promotes the growth and migration of trophoblasts by targeting AHNAK. *Eur Rev Med Pharmacol Sci* 2020, 24, 10954–9. doi:10.26355/eurrev_202011_23578.

23. Ross JW, Ashworth MD, Stein DR, Couture OP, Tuggle CK, Geisert RD. Identification of differential gene expression during porcine conceptus rapid trophoblastic elongation and attachment to uterine luminal epithelium. *Physiol Genomics* 2009, 36, 140–8. doi:10.1152/physiolgenomics.00022.2008.

24. Wang W, Sung N, Gilman-Sachs A, Kwak-Kim J. T helper (Th) cell profiles in pregnancy and recurrent pregnancy losses: Th1/Th2/Th9/Th17/Th22/Tfh cells. *Front Immunol* 2020, 11, 2025. doi:10.3389/fimmu.2020.02025.

25. Sundararaj S, Ravindran A, Casarotto MG. AHNAK: The quiet giant in calcium homeostasis. *Cell Calcium* 2021, 96, 102403. doi:10.1016/j.ceca.2021.102403.

26. Chen B, Wang J, Dai D, Zhou Q, Guo X, Tian Z, et al. AHNAK suppresses tumour proliferation and invasion by targeting multiple pathways in triple-negative breast cancer. *J Exp Clin Cancer Res* 2017, 36, 65. doi:10.1186/s13046-017-0522-4.

27. Liu ZM, Yang XL, Jiang F, Pan YC, Zhang L. Matrine involves in the progression of gastric cancer through inhibiting miR-93-5p and upregulating the expression of target gene AHNAK. *J Cell Biochem* 2020, 121, 2467–77. doi:10.1002/jcb.29469.

28. Comins-Boo A, Cristobal I, Fernandez-Arquero M, Rodriguez de Frias E, Calvo Urrutia M, Pilar Suarez L, et al. Functional NK surrogate biomarkers for inflammatory recurrent pregnancy loss and recurrent implantation failure. *Am J Reprod Immunol* 2021, 86, e13426. doi:10.1111/aji.13426.

29. Zhan X, Fu Q, He Q, Dong Q, Xie J, Geng Y, et al. The role of cyclic GMP-AMP synthase and interferon-I-inducible protein 16 as candidate biomarkers of systemic lupus erythematosus. *Clin Chim Acta* 2021, 524, 69–77.

30. Jeong J, Lee HK. The role of CD4(+) T cells and microbiota in the pathogenesis of asthma. *Int J Mol Sci* 2021, 22,11822.

31. Zolfaghari MA, Arefnezhad R, Parhizkar F, Hejazi MS, Motavalli Khiavi F, Mahmoodpoor A, et al. T lymphocytes and preeclampsia: the potential role of T-cell subsets and related MicroRNAs in the pathogenesis of preeclampsia. *Am J Reprod Immunol* 2021, 86, e13475. doi:10.1111/aji.13475.

32. He Y, Fang Y, Zhai B, Liu X, Zhu G, Zhou S, et al. Gm40600 promotes CD4(+) T-cell responses by interacting with AHNAK. *Immunology* 2021, 164, 190–206. doi:10.1111/imm.13365.

33. Eriksson AM, Leikfoss IS, Abrahamsen G, Sundvold V, Isom MM, Keshari PK, et al. Exploring the role of the multiple sclerosis susceptibility gene CLEC16A in T cells. *Scand J Immunol* 2021, 94, e13050. doi:10.1111/sji.13050.

34. Fu J, Shi H, Wang B, Zhan T, Shao Y, Ye L, et al. LncRNA PVT1 links Myc to glycolytic metabolism upon CD4(+) T cell activation and Sjogren's syndrome-like autoimmune response. *J Autoimmun* 2020, 107, 102358. doi:10.1016/j.jaut.2019.102358.

35. Prairie E, Cote F, Tsakpinoglou M, Mina M, Quiniou C, Leimert K, et al. The determinant role of IL-6 in the establishment of inflammation leading to spontaneous preterm birth. *Cytokine Growth Factor Rev* 2021, 59, 118–30. doi:10.1016/j.cytogfr.2020.12.004.

36. Figueiredo AS, Schumacher A. The T helper type 17/regulatory T cell paradigm in pregnancy. *Immunology* 2016, 148, 13–21. doi:10.1111/imm.12595.

37. Muyayalo KP, Li ZH, Mor G, Liao AH. Modulatory effect of intravenous immunoglobulin on Th17/Treg cell balance in women with unexplained recurrent spontaneous abortion. *Am J Reprod Immunol* 2018, 80, e13018. doi:10.1111/aji.13018.

38. Granne I, Shen M, Rodriguez-Caro H, Chadha G, O'Donnell E, Brosens JJ, et al. Characterisation of peri-implantation endometrial Treg and identification of an altered phenotype in recurrent pregnancy loss. *Mucosal Immunol* 2021, 15, 120–129.

39. Abdolmohammadi Vahid S, Ghaebi M, Ahmadi M, Nouri M, Danaei S, Aghebati-Maleki L, et al. Altered T-cell subpopulations in recurrent pregnancy loss patients with cellular immune abnormalities. *J Cell Physiol* 2019, 234, 4924–33. doi:10.1002/jcp.27290.

40. Shahbazi MN, Wang T, Tao X, Weatherbee BAT, Sun L, Zhan Y, et al. Developmental potential of aneuploid human embryos cultured beyond implantation. *Nat Commun* 2020, 11, 3987. doi:10.1038/s41467-020-17764-7.

41. Mackay CA, Smit JS, Khan F, Dessai F, Masekela R. IL-6 predicts poor early post-natal growth in very low-birth-weight infants in a low-middle income setting. *J Trop Pediatr* 2021, 67, fmaa132.

42. Khosravi N, Badamchi A, Khalesi N, Tabatabaee A, Naghdalipour M, Asgarian R. Measurement of interleukin-6 (IL-6) and erythropoietin (EPO) in umbilical cords of preterm infants with intraventricular hemorrhage in two hospitals in Tehran. *J Matern Fetal Neonatal Med* 2017, 30, 1847–50. doi:10.1080/14767058.2016.1228055.

43. Roose JP, Diehn M, Tomlinson MG, Lin J, Alizadeh AA, Botstein D, et al. T cell receptor-independent basal signaling via Erk and Abl kinases suppresses RAG gene expression. *PLoS Biol* 2003, 1, E53. doi:10.1371/journal.pbio.0000053.

44. da Silva TA, Oliveira-Brito PKM, Goncalves TE, Vendruscolo PE, Roque-Barreira MC. ArtinM mediates murine T cell activation and induces cell death in Jurkat human leukemic T cells. *Int J Mol Sci* 2017, 18, 1400.